CrystEngComm

Accepted Manuscript

This is an *Accepted Manuscript*, which has been through the Royal Society of Chemistry peer review process and has been accepted for publication.

Accepted Manuscripts are published online shortly after acceptance, before technical editing, formatting and proof reading. Using this free service, authors can make their results available to the community, in citable form, before we publish the edited article. We will replace this *Accepted Manuscript* with the edited and formatted *Advance Article* as soon as it is available.

You can find more information about *Accepted Manuscripts* in the Information for Authors.

Please note that technical editing may introduce minor changes to the text and/or graphics, which may alter content. The journal's standard Terms & Conditions and the Ethical guidelines still apply. In no event shall the Royal Society of Chemistry be held responsible for any errors or omissions in this *Accepted Manuscript* or any consequences arising from the use of any information it contains.

ROYAL SOCIETY OF CHEMISTRY

www.rsc.org/crystengcomm

Please do not adjust margins

Journal Name

ARTICLE

Tailoring the Photocatalytic Activity of Layered Perovskites by Opening the Interlayer Vacancy *via* Ion-exchange Reactions

Received 00th January 20xx,
Accepted 00th January 20xx

DOI: 10.1039/x0xx00000x

www.rsc.org/

Yingqi Wang,[ab] Xiaofang Lai,[b] Xujie Lü,*[c] Yanting Li,[d] Qinglong Liu,[b] Jianhua Lin,[b] and Fuqiang Huang*[bc]

Layer-structured materials have shown great promising in photocatalytic applications. The criteria for effective design and selecting of superior layered photocatalysts according to their crystal structures is extremely important. Herein, a series of layered perovskite $MLa_2Ti_3O_{10}$ (*M* = Ca, Sr, Ba) and $K_{2x}Ca_{1-x}La_2Ti_3O_{10}$ (*x* = 0.05, 0.11, 0.25) were prepared by an ion-exchange approach from $K_2La_2Ti_3O_{10}$. Their photocatalytic properties were evaluated by degradation of methyl orange (MO), phenol and photocatalytic hydrogen evolution. Their catalytic activities were significantly improved compared to $K_2La_2Ti_3O_{10}$, in the order of Ca>Sr>Ba>K for both organic pollutant degradation and H_2 evolution. The optimized composition of $K_{2x}Ca_{1-x}La_2Ti_3O_{10}$ with *x* = 0.11 shows an increase of four times in photocatalytic efficiency in comparison to pristine $K_2La_2Ti_3O_{10}$. The underlying mechanism of the improved performance is discussed in detail in terms of the packing factor model, which demonstrates that a more open structure with lower packing factor possesses higher photocatalytic activity in the layered perovskites.

Introduction

Photocatalytic pollutant degradation and hydrogen evolution, which will lead to a promising and low-cost solution to the environmental and energy issues, have received continuous attention over decades.[1-8] The main process of photocatalytic reactions include light absorption by the semiconductor photocatalysts, generation, separation, or recombination of photo-excited charges (electrons and holes) and then charge transfer to the reactants.[9, 10] The built-in electric fields between the layers for layered compounds are favorable for electron-hole (e^-–h^+) separation and transport, which contribute to a higher photocatalytic efficiency.[11] In addition, previous studies have shown that photocatalytic oxidative and reductive reaction sites are spatially separated in some layered photocatalysts.[12, 13] This could retard the recombination of photogenerated electron-holes and lead to improved photocatalytic activity. Many semiconductors with layered structures show outstanding photocatalytic properties, such as $Sr_2Nb_2O_7$, $La_2Ti_2O_7$, $RbLaNb_2O_7$, $K_2La_2Ti_3O_{10}$,[14-18] whose performance is closely related to the interlayer space.[19, 20]

A simple model based on the crystal packing factor (PF), which is computed by dividing the sum of spherical ion or atom volumes by the unit-cell volume, was proposed to evaluate the photocatalytic activity. The rationality and feasibility of the packing factor model can be expected, but just few studies have provided direct evidence so far.[21, 22] The difficulty originates from the complexity of photocatalytic reactions, for example, the performance is highly dependent on the synthetic methods. Hence, it's very critical to choose a rational method to prepare a series of samples for comparison. Ion-exchange reaction, as a simple and effective way to tailor the inter layer, could be a good choice to study the relationship between the inter layer space and photocatalytic properties. Because all the catalysts were prepared by exchange from the same starting material, other influence factors such as surface area and morphology effects could be excluded. $K_2La_2Ti_3O_{10}$, as an excellent layered photocatalyst, has arisen extensive interest.[9, 12] The diavalent alkali earth ions exchange of K^+ in $K_2La_2Ti_3O_{10}$ was investigated and their photocatalytic properties were evaluated.

In this work, a series of layered perovskite $MLa_2Ti_3O_{10}$ (*M* = Ca, Sr, Ba) and $K_{2x}Ca_{1-x}La_2Ti_3O_{10}$ (*x* = 0, 0.05, 0.11, 0.25) were prepared by metathesis reaction from $K_2La_2Ti_3O_{10}$. In these layered perovskites, Ti-O octahedron acts as the active photocatalytic center, while La^{3+} and interlayer K^+, M^{2+} is the photocatalytic inert part but modulate the structure relation between Ti-O octahedral. For $MLa_2Ti_3O_{10}$ series, the photocatalytic activities ordered as Ca>Sr>Ba; in the $K_{2x}Ca_{1-x}La_2Ti_3O_{10}$ (*x* = 0, 0.05, 0.11, 0.25, 1) series, the sample with *x* = 0.11 showed the best performance. The difference in activities

[a] Department of Materials Science and Engineering, College of Engineering, Peking University, Beijing 100871 , P. R. China
[b] Beijing National Laboratory for Molecular Sciences and State Key Laboratory of Rare Earth Materials Chemistry and Applications,College of Chemistry and Molecular Engineering, Peking University, 202 Chengfu Road, Beijing 100871, P. R. China. E-mail: huangfq@pku.edu.cn
[c] CAS Key Laboratory of Materials for Energy Conversion, Shanghai Institute of Ceramics, Chinese Academy of Sciences, 1295 Dingxi Road, Shanghai 200050, P. R. China. E-mail: mselxj@gmail.com
[d] School of Materials Science and Engineering, Shijiazhuang Tiedao University, Shijiazhuang 050043, China

† Electronic Supplementary Information (ESI) available: Synthesis, crystallography data and photoluminescence spectra. See DOI: 10.1039/x0xx00000x

CrystEngComm Accepted Manuscript

Please do not adjust margins

of these compounds was discussed in detail in terms of packing factor model[21, 22] and further supported by photoluminescence results. Our findings directly demonstrate that a more open structure with lower packing factor possesses higher photocatalytic activity in the layered perovskites.

Experimental Section

Synthetic procedures

The $K_2La_2Ti_3O_{10}$ powders were synthesized by the polymerized complex (PC) method as reported in the literature.[17] $MLa_2Ti_3O_{10}$ (M = Ca, Sr, Ba) were prepared by ion exchange reaction of $K_2La_2Ti_3O_{10}$ in excessive MCl_2 at 973K (M = Ca) or 1023K (M = Sr, Ba) for 48h with one intermediate washing, adding new MCl_2 and grinding. The resultants were washed with deionized water and dried in air. $K_{2x}Ca_{1-x}La_2Ti_3O_{10}$ (x = 0.05, 0.11, 0.25) series were prepared by ion exchange of $K_2La_2Ti_3O_{10}$ in excessive $CaCl_2$/KCl eutectic salt at 973K for 48h. The molar ratio of $CaCl_2$/KCl was 8:1, 4:1, and 2:1 respectively.

Characterization

Optical diffuse-reflectance measurements were carried out with a Hitachi UV-4100 spectrophotometer. The PXRD tests were carried out on a Bruker D2 Phaser X-ray diffractometer (Cu Kα). PL measurements were carried out on Hitachi F-7000 fluorescence spectrophotometer at room temperature. The compositions of $K_{2x}Ca_{1-x}La_2Ti_3O_{10}$ series were determined by means of an inductively coupled plasma (ICP) atomic emission spectrophotometer (Leeman, PROFILE SPEC). Samples for ICP were dissolved in heated HNO_3. The Brunauer–Emmett–Teller (BET) specific surface areas (SSAs) were determined through nitrogen adsorption at 77 K using a Micromeritics ASAP2010 instrument.

Photocatalytic activity measurement

In all catalytic experiments, the reaction temperature was kept at room temperature by using a circulating water jacket. The catalytic reaction for the degradation of 30 mg/L MO aqueous solution was carried out in an inner irradiated quartz cell with a 500 W high-pressure mercury lamp. 0.3g of catalyst was added into 300ml of MO solution. UV illumination was conducted after the suspension was magnetically stirred in dark for 50 min. During irradiation, about 5ml suspension was continually taken from the reaction cell at given time intervals for subsequent MO concentration analysis after centrifuging. In the case of the phenol degradation, the experimental conditions are same as the MO degradation except for the concentrations of phenol aqueous solution (40 mg/L). The concentration of phenol was determined by previously reported method.[23]

Ni-loaded samples were used for photocatalytic hydrogen evolution test according to the literature.[17] Photocatalytic hydrogen evolution was performed in a side irradiation quartz cell. The aqueous solution contained 10% methanol as sacrificial reagent. The catalyst concentration was 0.1g per 100ml solution. A 400 W Xe lamp was used as the light source. Hydrogen evolved was analyzed by an online thermal conductivity detector (TCD) gas chromatograph.

Results and discussion

Structural characterization

Two series of derivatives, $MLa_2Ti_3O_{10}$ (M = Ca, Sr, Ba) and $K_{2x}Ca_{1-x}La_2Ti_3O_{10}$ (x = 0.05, 0.11, 0.25) were synthetized via ion-exchange reactions with $K_2La_2Ti_3O_{10}$:

$$K_2La_2Ti_3O_{10} + MCl_2 \rightarrow 2KCl + MLa_2Ti_3O_{10} \quad (1)$$

$$K_2La_2Ti_3O_{10} + (1-x)CaCl_2 \rightarrow (2-2x)KCl + K_{2x}Ca_{1-x}La_2Ti_3O_{10} \quad (2)$$

The structure of $K_2La_2Ti_3O_{10}$ is composed of a perovskite unit with tree layers and a rock-salt unit of potassium ion stacked alternately along the c-axis. The adjacent triple perovskite sheets, $La_2Ti_3O_{10}^{2-}$, are stacked with a displacement by 1/2 along the (110) direction. The framework of the perovskite layer of the ion-exchanged products is the same as those of the corresponding potassium compound, which is constructed of triple perovskite layer. But the lower density of inter layer ion results in different perovskite layer displacement and decreased of crystal symmetry. [24, 25]

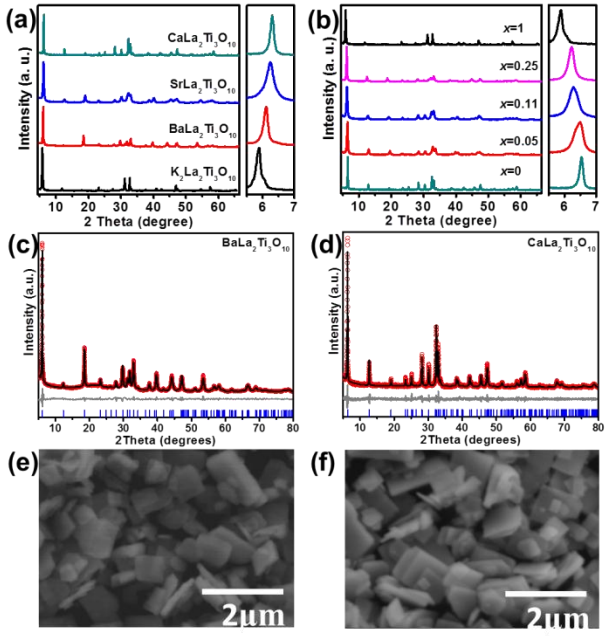

Figure 1 The XRD patterns of (a) $MLa_2Ti_3O_{10}$ (M = Ca, Sr, Ba) and (b) $K_{2x}Ca_{1-x}La_2Ti_3O_{10}$ (x = 0, 0.05, 0.11, 0.25, 1). X-ray powder pattern refinement for (c) $BaLa_2Ti_3O_{10}$. (d) $CaLa_2Ti_3O_{10}$. The calculated and observed patterns are shown on the top by the black solid line and the red dots, respectively. The trace in the middle is a plot of the difference between the calculated and the observed intensities. SEM images of $K_2La_2Ti_3O_{10}$ (e) before and (f) after Ca^{2+} exchange.

The complete or partial substitution of potassium by alkali earth M (M = Ca, Sr, Ba) was confirmed by energy-dispersive spectrum (EDS), given a stoichiometric composition of M : La : Ti = 1 : 2 : 3 within experimental errors. The formulas of the partially substituted sample were determined by the Inductive

CrystEngComm Accepted Manuscript

This journal is © The Royal Society of Chemistry 20xx

Table 1 Crystallographic Data of $BaLa_2Ti_3O_{10}$ and $CaLa_2Ti_3O_{10}$

	Atom	site	*x*	*y*	*z*	Occ	Beq
$BaLa_2Ti_3O_{10}$ *C* 222 *a* = 3.8279(2) *b* = 28.514(2) *c* = 3.8753(1) R_{wp} = 12.23 R_p = 9.50	Ba	4*g*	0	0.2319(9)	0	0.5	0.4(1)
	La	4*g*	0	0.0732(2)	0	1	0.4(1)
	Ti1	2*c*	0.5	0	0.5	1	0.4(1)
	Ti2	4*h*	0	0.3619(4)	0.5	1	0.4(1)
	O1	2*d*	0	0	0.5	1	1.3(3)
	O2	4*h*	0	0.1272(9)	0.5	1	1.3(3)
	O3	4*h*	0	0.3046(6)	0.5	1	1.3(3)
	O4	4*g*	0	0.3646(7)	0	1	1.3(3)
	O5	4*h*	0	0.4367(8)	0.5	1	1.3(3)
	O6	2*b*	0	0.5	0	1	1.3(3)
$CaLa_2Ti_3O_{10}$ *P* nnm *a* = 3.8989(3) *b* = 27.908(2) *c* = 3.7851(2) R_{wp} = 13.23 R_p = 10.61	Ti1	2*a*	0	0	0	1	0.4(1)
	Ti2	4*g*	0.014(6)	0.1491(3)	0	1	0.4(1)
	La	4*g*	-0.009(2)	0.4242(1)	0	1	0.4(1)
	Ca	4*g*	0.049(8)	0.2876(6)	0	0.5	0.4(1)
	O1	2*b*	0	0	0.5	1	1.4(3)
	O2	2*d*	0	0.5	0.5	1	1.4(3)
	O3	4*g*	-0.070(9)	0.0727(8)	0	1	1.4(3)
	O4	4*g*	0.440(9)	0.129 (2)	0	1	1.4(3)
	O5	4*g*	0.564(9)	0.363 (2)	0	1	1.4(3)
	O6	4*g*	-0.081(8)	0.210(1)	0	1	1.4(3)

Coupled Plasma Emission Spectrometer (ICP) approach. The conservation of perovskite layer during metathesis reaction was confirmed by powder X-ray diffraction (XRD). The XRD patterns of $MLa_2Ti_3O_{10}$ (*M* = Ca, Sr, Ba) and $K_{2x}Ca_{1-x}La_2Ti_3O_{10}$ (*x* = 0, 0.05, 0.11, 0.25, 1) are shown in Figure 1a&b. The patterns of $MLa_2Ti_3O_{10}$ could be indexed into orthorhombic structure, lower than the tetragonal crystal symmetry of the parent compound $K_2La_2Ti_3O_{10}$.[25, 26] The lattice parameters were acquired from experimental data and listed in Table S2. The XRD pattern of $MLa_2Ti_3O_{10}$ was in close similarity with each other, but the splitting of peaks and emergence of extincted peaks indicated the decreasing in symmetry. Structural analysis through Rietveld refinement was carried out. The crystallography data of $MLa_2Ti_3O_{10}$ (*M* = Ca, Ba) were summarized in Table 1. $SrLa_2Ti_3O_{10}$ and $K_{2x}Ca_{1-x}La_2Ti_3O_{10}$, are isostructure to $BaLa_2Ti_3O_{10}$ and Ca $La_2Ti_3O_{10}$ respectively. The observed and calculated patterns of $MLa_2Ti_3O_{10}$ (*M* = Ca, Ba) are shown in Figure 1. The lattice parameters and relative peak intensity in PXRD pattern of $BaLa_2Ti_3O_{10}$ are slightly differed from $BaLa_2Ti_3O_{10}$ synthesis by conventional solid state reaction.[27] In high temperature solid state reaction, Ba^{2+} and La^{3+} are totally disordered. In the low temperature ion exchange process, the $La_2Ti_3O_{10}^{2-}$ layer is preserved and the disorder of La^{3+} and Ba^{2+} is suppressed. Layered $CaLa_2Ti_3O_{10}$ and $SrLa_2Ti_3O_{10}$ synthesized by traditional solid state reaction have not been reported. When alkali ion is exchanged by divalent alkali earth ion, one vacancy per exchanged cation is introduced, resulting in a more capacious interlayer space. The lowing of packing density in crystal may lower the elastic stiffness, increase the internal field and improve charge mobility, which directly affects the photocatalytic properties.[22] The morphology of pristine $K_2La_2Ti_3O_{10}$ and Ca^{2+} exchanged product are shown in Figu 1e&f. All the samples prepared via ion-exchange reaction have similar morphology, size, and BET surface area (listed in Table 2 and Table 3).

UV-Vis DRS analysis

The UV-vis diffuse reflectance spectra of $MLa_2Ti_3O_{10}$ (*M* = Ca, Sr, Ba) and $K_{2x}Ca_{1-x}La_2Ti_3O_{10}$ (*x* = 0.05, 0.11, 0.25) are shown in Figure 2. It can be observed that the light absorption starts at about 350 nm. For an indirect semiconductor, the optical absorption has the following behavior near the band edge:[28]

$$\alpha(h\nu) = A(h\nu - E_g)^{n/2} \quad (3)$$

α, ν, E_g, and A are absorption coefficient, light frequency, band gap, and constant, respectively, and n depends on the characteristics of the transition. Kubelka-Munk function F(R) is proportional to the absorption coefficient $\alpha(h\nu)$.[29, 30] Presumably, $MLa_2Ti_3O_{10}$ (*M* = Ca, Sr, Ba) and $K_{2x}Ca_{1-x}La_2Ti_3O_{10}$ (*x* = 0.05, 0.11, 0.25) have the similar nature with the pare t $K_2La_2Ti_3O_{10}$, showing indirect band gap character. [31] Their band gaps (E_g) were estimated from the plot of $F(R)^{1/2}$ versus $h\nu$ (Figure 2), given in Table 2 and Table 3.

The absorption edges of $K_{2x}Ca_{1-x}La_2Ti_3O_{10}$ (*x* = 0, 0.05, 0.11, 0.25, 1) are almost the same with each other. A red-shift of the band edge of $SrLa_2Ti_3O_{10}$ can be observed in the DRS of $MLa_2Ti_3O_{10}$ (*M* = K_2, Ca, Sr, Ba). A possible explanation of this

CrystEngComm Accepted Manuscript

red shift is that the ionic radii of Sr^{2+} is much closer to La^{3+} and a little bit Sr^{2+} may take place La^{3+}. All compound investigated in this work have similar band gap around 3.1-3.4 eV, indicating that the light absorption ability is not the main source of improvement in photocatalytic performance.

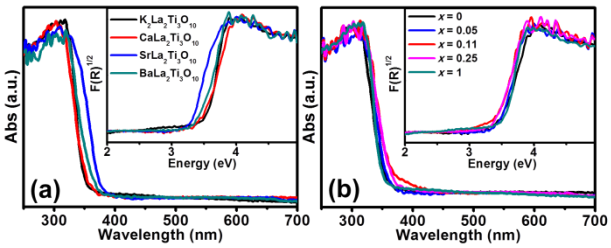

Figure 2 UV-vis diffuse reflectance spectra of (a) MLa$_2$Ti$_3$O$_{10}$ (M = K, Ca, Sr, Ba) and (b) K$_{2x}$Ca$_{1-x}$La$_2$Ti$_3$O$_{10}$ (x = 0, 0.05, 0.11, 0.25, 1). The inset shows the corresponding plots of F(R)$^{1/2}$ vs hv for the determination of band gap.

Photocatalytic pollutant degradation and hydrogen evolution

The photocatalytic activities of this series of Dion-Jacobson phase were first evaluated by the decomposition of organic dye under the visible-light irradiation. The Methyl Orange (MO) degradation reaction was chosen as a probe for the characterization of its photocatalytic property. MO is a chemically-stable dye with the maximum absorption at 464 nm, associated with the azo bond (-N=N-), and is widely used as a facile way to monitor the effect of photocatalytic performance. Figure 3a, 3b shows the concentration evolution of MO degradation under different catalyst. CaLa$_2$Ti$_3$O$_{10}$ exhibited the best photocatalytic activity in MLa$_2$Ti$_3$O$_{10}$ (M = K, Ca, Sr, Ba) series. More than 80% of MO was degraded within 18 min. The order of photocatalytic activity was Ca>Sr>Ba>K. The photocatalytic activity of MO degradation over partially divalent ion exchanged product, K$_{2x}$Ca$_{1-x}$La$_2$Ti$_3$O$_{10}$ (x = 0, 0.05, 0.11, 0.25, 1), also showed significant improvement compared to the parent K$_2$La$_2$Ti$_3$O$_{10}$. With the degree of divalent Ca^{2+} exchanging into the site of K^+, the rate coefficient of photocatalytic degradation of MO first increased, reaching a maximum around x = 0.11and then degreased, but the reaction rate is still much higher than that of the parent compound K$_2$La$_2$Ti$_3$O$_{10}$.

Then, the photocatalytic degradation of colorless phenol under UV-light irradiation has also been examined. It can be clearly seen from Figure 3c, 3d that the photocatalytic performance is significantly improved after alkali earth ion-exchange, and the partially ion-exchanged material K$_{0.22}$Ca$_{0.89}$La$_2$Ti$_3$O$_{10}$ still exhibit the highest photocatalytic activity for phenol degradation, which is consistent with the experimental results of MO degradation.

The photocatalytic activities of organic pollutant degradation are closely related to the oxidation ability of photo-generated holes in semiconductor catalyst. While the photocatalytic hydrogen evolution is highly correlated with the reduction ability of photo-generated electrons. The photocatalytic hydrogen evolution in aqueous solution containing methanol as a sacrificial reagent for h^+ capture were also measured. The hydrogen evolutions over MLa$_2$Ti$_3$O$_{10}$ (M = K, Ca, Sr, Ba) and K$_{2x}$Ca$_{1-x}$La$_2$Ti$_3$O$_{10}$ (x = 0, 0.05, 0.11, 0.25, 1) are shown in Figure 3e, 3f. The activity sequence were shown as Ca>Sr>Ba>K, the same as that for MO and phenol degradation described above. These results demonstrated that the improved photocatalytic activities result from the enhanced charge separation and transport in the catalysts with more open structure. After MO degradation or H_2 evolution reactions, the crystal structures of MLa$_2$Ti$_3$O$_{10}$ (M = K, Ca, Sr, Ba) and K$_{2x}$Ca$_{1-x}$La$_2$Ti$_3$O$_{10}$ (x = 0, 0.05, 0.11, 0.25, 1) were checked again by X-ray diffraction. It was found that the semiconductor remains the same crystal structure after ptotocatalytic reactions.

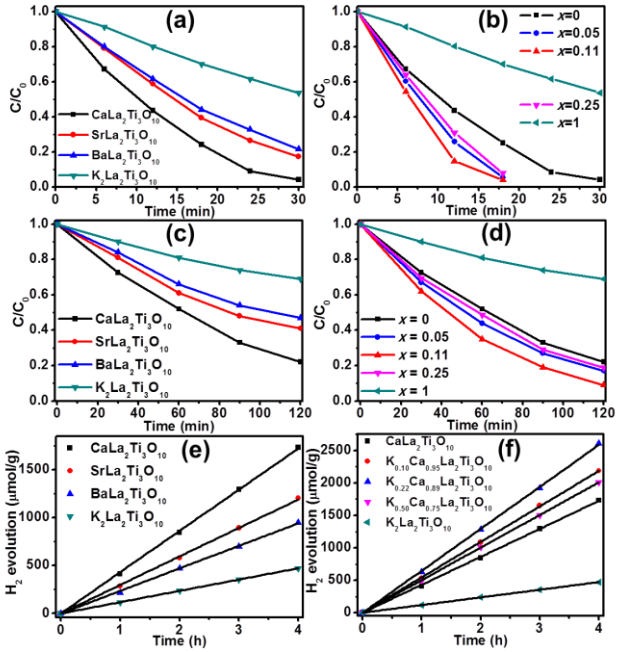

Figure 3 MO degradation over (a) MLa$_2$Ti$_3$O$_{10}$ (M = K, Ca, Sr, Ba) and (b) K$_{2x}$Ca$_{1-x}$La$_2$Ti$_3$O$_{10}$ (x = 0, 0.05, 0.11, 0.25, 1). Phenol degradation over (c) MLa$_2$Ti$_3$O$_{10}$ (M = K, Ca, Sr, Ba) and (d) K$_{2x}$Ca$_{1-x}$La$_2$Ti$_3$O$_{10}$ (x = 0, 0.05, 0.11, 0.25, 1). Photocatalytic hydrogen evolutions over (e) MLa$_2$Ti$_3$O$_{10}$ (M = K, Ca, Sr, Ba) and (f) K$_{2x}$Ca$_{1-x}$La$_2$Ti$_3$O$_{10}$ (x = 0, 0.05, 0.11, 0.25, 1).

Detailed explanation for the improved performance

To understand what determines the photocatalytic activity sequence for the MLa$_2$Ti$_3$O$_{10}$ (M = K, Ca, Sr, Ba) and K$_{2x}$Ca$_{1-x}$La$_2$Ti$_3$O$_{10}$ (x = 0, 0.05, 0.11, 0.25, 1), a series of factors are examined, such as surface area, morphology, electronic structure, and crystal structure. Surface area and morphology are among the key factors for catalyst, all the catalyst in this research are synthesis from the same parent layered perovskite, K$_2$La$_2$Ti$_3$O$_{10}$ via ion exchange process, so they exhibit similar morphology and surface area as shown in Figure 1, Table 2 and Table 3. Band gap affect the amount of light absorption, thus influence the photocatalytic activities. Since the bandgap of MLa$_2$Ti$_3$O$_{10}$ (M = K, Ca, Sr, Ba) and K$_{2x}$Ca$_{1-x}$La$_2$Ti$_3$O$_{10}$ (x = 0, 0.05, 0.11, 0.25, 1) series are all similar, the contribution from the difference in absorption is less than 10%

CrystEngComm Accepted Manuscript

This journal is © The Royal Society of Chemistry 20xx

Electronic structures of a semiconductor also greatly influence the catalytic activity through the mobility, separation, redox ability of electrons and holes. The valance band (VB) of $K_{2x}M_{1-x}La_2Ti_3O_{10}$ (*M* = Ca, Sr, Ba; *x* = 0, 0.05, 0.11, 0.25, 1) is dominated by O *2p* states and the conduction band (CB) is mainly originated from Ti *3d* and *4S* states, the exchange of interlayer alkali by alkaline-earth metal have little effect on the band structure near Fermi level. Ti-O octahedral can be regarded as the photocatalytic active center, while the interlayer alkali or alkaline-earth metal ion is photocatalytic inert and serve as structural supporter. Therefore, it seems that $K_{2x}M_{1-x}La_2Ti_3O_{10}$ series do not show much difference in energy bands near the VBM and CBM regions. Since valence band of these photocatalysts is dominated by O *2p* states, oxygen vacancy may have an impact on the photocatalytic activity. According to previous studies, the vacant oxygen site can cause redistribution of excess electrons and neighboring atoms, and thus electron state will be introduced near the valence band edge, resulting in a red shift of optical absorption edge or enhanced visible light absorption.[1, 7, 32, 33] However, the absorption spectra in our sample remain unchanged. This indicates that there is no obvious change of oxygen deficiencies in the series of photocatalysts. In addition, all of these samples were synthesized in air without any protection, so the oxygen vacancies would not be preferred. Thus, the contribution of oxygen defects on the photocatalytic activity in our system can be excluded.

All of the influence factors mentioned above can be excluded in our cases, it is probable that the different photocatalytic activities are related to crystal structural factors only. One proposed model invokes that ionic distortion and lowering in symmetry may generate local electrical field or dielectric polarization that benefits charge transport and electron-hole separation.[21, 34, 35] This may account for the superior photocatalytic activity of monoclinic or orthorhombic $MLa_2Ti_3O_{10}$ (*M* = Ca, Sr, Ba) to tetragonal $K_2La_2Ti_3O_{10}$, but the different activity of monoclinic $K_{2x}Ca_{1-x}La_2Ti_3O_{10}$ (*x* = 0, 0.05, 0.11, 0.25) and $MLa_2Ti_3O_{10}$ (*M* = Ca, Sr) remain implicit.

More recently, based on the survey of a series of inorganic oxides containing d^{10} of d^0 cations, a model for the evaluation of photocatalytic activity has been proposed.[21, 36] According to this model, lower crystal packing factor (PF) is correlated to better photocatalytic performance in photocatalytic semiconductor of similar structure or chemistry. The packing factor of a compound is calculated by dividing the sum of spherical ion volumes by the unit cell volume, assuming spherical ions with a Shannon radius[37] that depends on the coordination number. According to the reference, the intrinsic relation between lower PF factor and higher photocatalytic activities involve the lifetime and mobility of electrons and holes. Photocatalytic active ion in a lower PF structure is more polarizable, results in larger exciton radius and prolonged lifetimes of electrons and holes. Meanwhile, a lower PF structure is more deformable, which lowers the activation (hopping) barrier for polarons, thus increases their mobility. The PF factor of $MLa_2Ti_3O_{10}$ (M = K_2, Ca, Sr, Ba) and $K_{2x}Ca_{1-x}La_2Ti_3O_{10}$ (*x* = 0.05, 0.11, 0.25) were listed in Table 2 and Table 3. A correlation between photocatalytic activity and PF factor was shown in Figure 4, exhibiting a linear relationship. The compound with lower PF shows better photocatalytic activity. In our systems, when the univalent alkali ion is replaced by divalent alkali earth ion, in order for the charge balance, one vacancy per exchanged cation is introduced. This process opened the structure to a more capacious interlayer space, provided wider spatial location for vibrations, and led to a higher momentary polarizing field that promote e^--h^+ separation, thus benefitted the photocatalytic activities. In order to confirm the difference in electron-hole separation and recombination, photo luminescence spectra were recorded (Figure S2 in ESI), since the PL intensity is related to electron-hole recombination rate. If other factors remained unchanged, a lower PL intensity may indicate slower recombination, leading to longer life time of electron-hole pairs.[38-40] The PL intensities show the reserved order of Ca<Sr<Ba<K, further evidence the intrinsic relation between lower PF and higher photocatalytic activity.

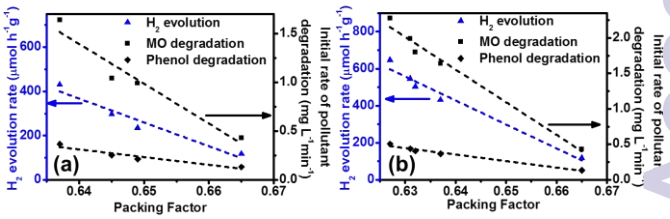

Figure 4 Dependence of photocatalytic activity on the packing factor for (a) $MLa_2Ti_3O_{10}$ (*M* = K_2, Ca, Sr, Ba) and (b) $K_{2x}Ca_{1-x}La_2Ti_3O_{10}$ (*x* = 0, 0.05, 0.11, 0.25, 1).

The PF of $K_{2x}Ca_{1-x}La_2Ti_3O_{10}$ first decrease and then increase with the expanding of exchanging ratio *x*, so the packing factor reach a minimum around *x* = 0.11. A visualized explanation is that, replacing two K^+ ion with one much smaller Ca^{2+} ion can making the interlayer space more capacious; the best state is not all the K^+ were exchanged by Ca^{2+}, but a little K^+ remained between the perovskite layer. Because K^+ is larger in radius than Ca^{2+}, they can act as an ionic pillar to create larger interlayer space than pure Ca^{2+} species. So the partially exchanged product $K_{0.22}Ca_{0.89}La_2Ti_3O_{10}$ shows enhanced photocatalytic activity.

CrystEngComm Accepted Manuscript

Table 2 Cell parameters, PF factor, BET surface area, photocatalytic H_2 evolution rate and photo-degradation of $MLa_2Ti_3O_{10}$ (M = K_2, Ca, Sr, Ba).

Catalysts	V (Å^3)	Packing Factor	Initial rate of MO/phenol degradation (mg·L^{-1}·min^{-1})	H_2 evolution rate (μmol·h^{-1}·g^{-1})	Surface area (m^2/g)	Band gap (eV)
$CaLa_2Ti_3O_{10}$	412	0.637	1.64/0.367	431	5.12	3.40
$SrLa_2Ti_3O_{10}$	415	0.645	1.04/0.253	298	4.46	3.14
$BaLa_2Ti_3O_{10}$	423	0.649	0.99/0.213	235	4.78	3.33
$K_2La_2Ti_3O_{10}$	448	0.665	0.43/0.133	118	5.31	3.43

Table 3 Cell parameters, PF factor, photocatalytic and pseudo-first order rate constants of MO photo-degradation over $K_{2x}Ca_{1-x}La_2Ti_3O_{10}$ (x = 0, 0.05, 0.11, 0.25, 1)

x	V (Å^3)	Packing Factor	Initial rate of MO/phenol degradation (mg·L^{-1}·min^{-1})	H_2 evolution rate (μmol·h^{-1}·g^{-1})	Surface area (m^2/g)	Band gap (eV)
0	412	0.637	1.64/0.367	431	5.12	3.40
0.05	418	0.631	1.99/0.440	546	4.93	3.35
0.11	424	0.627	2.28/0.507	647	4.34	3.27
0.25	429	0.632	1.80/0.407	503	5.27	3.26
1	448	0.665	0.43/0.133	118	5.31	3.43

Conclusions

The photocatalytic activity of tree-layered perovskite $K_2La_2Ti_3O_{10}$ was tailored by ion-exchange reaction with series of cations, Ca^{2+}, Sr^{2+}, Ba^{2+}. The photocatalytic performances of $MLa_2Ti_3O_{10}$ (M = K, Ca, Sr, Ba) follow the order of Ca>Sr>Ba>K, and $K_{2x}Ca_{1-x}La_2Ti_3O_{10}$ (x = 0, 0.05, 0.11, 0.25, 1) showed the best photocatalytic activity at x = 0.11. This sequence of photocatalytic performances is found to be related to a successively decrease in packing factor (PF). Lower PF leads to more capacious interlayer space, which benefits electron-hole transport and separation, resulting in improved photocatalytic performance. This work provides direct evidence for the rationality and feasibility of the packing factor model, which is an effective and sensitive criterion for developing superior photocatalysts with less guesswork.

Acknowledgements

This work was financially supported from NSF of China (Grant nos.61376056, 51125006, 91122034, 51121064), and Science and Technology Commission of Shanghai (Grant no. 13JC1405700, 14520722000).

Notes and references

1. X. Chen, L. Liu, P. Y. Yu and S. S. Mao, *Science*, 2011, 331, 746-750.
2. J. M. Herrmann, *Catalysis Today*, 1999, 53, 115-129.
3. G. Williams, B. Seger and P. V. Kamat, *Acs Nano*, 2008, 2, 1487-1491.
4. W. Li, Z. Wu, J. Wang, A. A. Elzatahry and D. Zhao, *Chemistry of materials*, 2014, 26, 287-298.
5. X. Lü, F. Huang, X. Mou, Y. Wang and F. Xu, *Advanced Materials*, 2010, 22, 3719-3722.
6. X. Lü, S. Ding, Y. Xie and F. Huang, *Eur. J. Inorg. Chem* 2011, 2011, 2879-2883.
7. T. Q. Lin, C. Y. Yang, Z. Wang, H. Yin, X. J. Lu, F. Q. Huang, J. H. Lin, X. M. Xie and M. H. Jiang, *Energy & Environmental Science*, 2014, 7, 967-972.
8. Z. Wang, C. Y. Yang, T. Q. Lin, H. Yin, P. Chen, D. Y. Wan, F. F. Xu, F. Q. Huang, J. H. Lin, X. M. Xie and M. H. Jiang, *Energy & Environmental Science*, 2013, 6, 3007-3014.
9. X. Chen, S. Shen, L. Guo and S. S. Mao, *Chemical Reviews*, 2010, 110, 6503-6570.
10. X. Lu, S. Ding, T. Lin, X. Mou, Z. Hong and F. Huang, *Dalton Trans.*, 2012, 41, 622-627.
11. X. Lin, F. Huang, W. Wang, Y. Wang, Y. Xia and J. Sh, *Applied Catalysis A: General*, 2006, 313, 218-223.
12. T. Takata, K. Shinohara, A. Tanaka, M. Hara, J. Kondo and K. Domen, *Journal of photochemistry and photobiology A: Chemistry*, 1997, 106, 45-49.
13. T. Takata, Y. Furumi, K. Shinohara, A. Tanaka, M. Hara, J. N. Kondo and K. Domen, *Chemistry of materials*, 1997, 9, 1063-&.
14. H. Kim, D. Hwang, Y. Kim and J. Lee, *Chemic Communications*, 1999, 1077-1078.
15. D. Arney and P. A. Maggard, *Acs Catalysis*, 2012, 2, 1711-1717.
16. J. Boltersdorf and P. A. Maggard, *Acs Catalysis*, 2013, 3, 2547-2555.

CrystEngComm Accepted Manuscript

This journal is © The Royal Society of Chemistry 20xx

Please do not adjust margins

17. S. Ikeda, M. Hara, J. N. Kondo, K. Domen, H. Takahashi, T. Okubo and M. Kakihana, *Chemistry of materials*, 1998, 10, 72-77.
18. J. Jiang, K. Zhao, X. Xiao and L. Zhang, *J. Am. Chem. Soc.*, 2012, 134, 4473-4476.
19. K. Sanjaya Ranmohotti, E. Josepha, J. Choi, J. Zhang and J. B. Wiley, *Advanced Materials*, 2011, 23, 442-460.
20. J.-H. Choy, H.-C. Lee, H. Jung and S.-J. Hwang, *J. Mater. Chem.*, 2001, 11, 2232-2234.
21. X. Lin, J. Wu, X. Lu, Z. Shan, W. Wang and F. Huang, *Physical chemistry chemical physics : PCCP*, 2009, 11, 10047-10052.
22. X. Lü, W. Yang, Z. Quan, T. Lin, L. Bai, L. Wang, F. Huang and Y. Zhao, *J. Am. Chem. Soc.*, 2013, 136, 419-426.
23. R. Su, R. Tiruvalam, Q. He, N. Dimitratos, L. Kesavan, C. Hammond, J. A. Lopez-Sanchez, R. Bechstein, C. J. Kiely and G. J. Hutchings, *Acs Nano*, 2012, 6, 6284-6292.
24. J. B. Goodenough and J. S. Zhou, *Chemistry of materials*, 1998, 10, 2980-2993.
25. A. Olsen and R. S. Roth, *J. Solid State Chem.*, 1985, 60, 347-357.
26. J. Gopalakrishnan, T. Sivakumar, K. Ramesha, V. Thangadurai and G. Subbanna, *J. Am. Chem. Soc.*, 2000, 122, 6237-6241.
27. L. Guo, H. Guo, G. Ma, M. Abbas and S. Gong, *Ceramics International*, 2012, 38, 4345-4352.
28. M. Fox, *Optical properties of solids*, Oxford University Press, New York, First edn., 2001.
29. G. Kortüm, W. Braun and G. Herzog, *Angewandte Chemie International Edition in English*, 1963, 2, 333-341.
30. X. Lü, X. Mou, J. Wu, D. Zhang, L. Zhang, F. Huang, F. Xu and S. Huang, *Adv. Funct. Mater.*, 2010, 20, 509-515.
31. Y. Huang, Y. Wei, S. Cheng, L. Fan, Y. Li, J. Lin and J. Wu, *Solar Energy Materials and Solar Cells*, 2010, 94, 761-766.
32. J. Wang, Z. Wang, B. Huang, Y. Ma, Y. Liu, X. Qin, X. Zhang and Y. Dai, *ACS Appl Mater Interfaces*, 2012, 4, 4024-4030.
33. C. Y. Yang, Z. Wang, T. Q. Lin, H. Yin, X. J. Lu, D. Y. Wan, T. Xu, C. Zheng, J. H. Lin, F. Q. Huang, X. M. Xie and M. H. Jiangl, *J. Am. Chem. Soc.*, 2013, 135, 17831-17838.
34. J. Wu, F. Huang, Z. Shan and Y. Wang, *Dalton Trans.*, 2011, 40, 6906-6911.
35. Z. Zou, J. Ye, K. Oka and Y. Nishihara, *Physical review letters*, 1998, 80, 1074.
36. Z. Shan, Y. Wang, H. Ding and F. Huang, *Journal of Molecular Catalysis A: Chemical*, 2009, 302, 54-58.
37. R. t. Shannon, *Acta Crystallographica Section A: Crystal Physics, Diffraction, Theoretical and General Crystallography*, 1976, 32, 751-767.
38. N. K. Veldurthi, G. Ravi, J. R. Reddy, S. Palla, N. R. Muniratnam, G. Prasad and M. Vithal, *Journal of the American Ceramic Society*, 2014, 97, 1829-1836.
39. G. Naresh and T. K. Mandal, *ACS applied materials & interfaces*, 2014, 6, 21000-21010.
40. S. Han, L. Hu, N. Gao, A. A. Al‐Ghamdi and X. Fang, *Adv. Funct. Mater.*, 2014, 24, 3725-3733.

CrystEngComm Accepted Manuscript

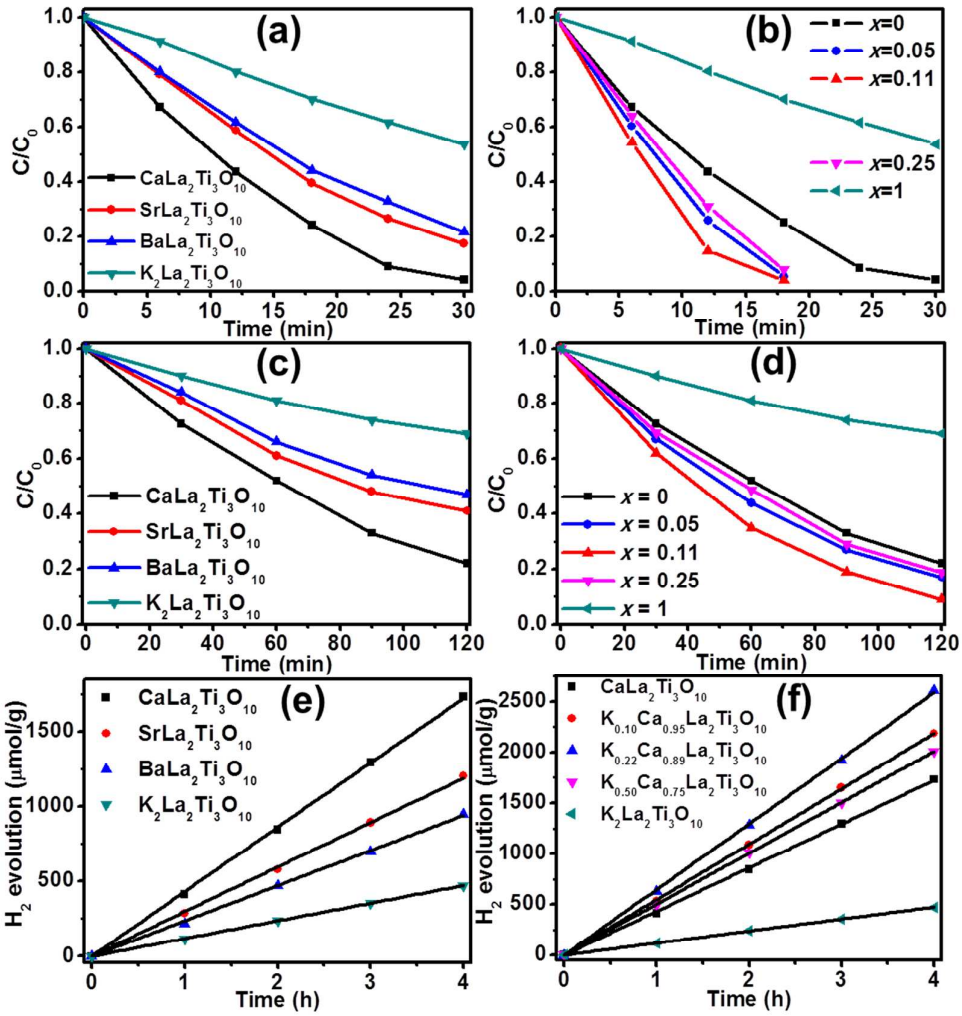

The photocatalytic activity of layered perovskite $K_2La_2Ti_3O_{10}$ was regulated by ion-exchange reaction with a series of cations, Ca^{2+}, Sr^{2+}, Ba^{2+}. The underlying mechanism of the improved performance and a effective model for designing photocatalyst were discussed.

CrystEngComm Accepted Manuscript